Hydrocracking of Fischer-Tropsch Waxes: Kinetic Modeling via LHHW Approach

Chiara Gambaro, Vincenzo Calemma, and Daniele Molinari
Eni Refining and Marketing, San Donato Research Center, 20097 San Donato Milanese, Italy

Joeri Denayer
Dept. of Chemical Engineering, Vrije Universiteit Brussel, Pleinlaan 2, B-1050 Brussel, Belgium

DOI 10.1002/aic.12291
Published online June 1, 2010 in Wiley Online Library (wileyonlinelibrary.com).

A lumped kinetic model to describe the hydrocracking of complex mixtures of paraffins, such as Fischer-Tropsch waxes, has been developed. A Langmuir-Hinshelwood-Hougen-Watson approach has been followed, accounting for physisorption by means of the Langmuir isotherm. Finally, a complete form of the rate expression is used, thus introducing the equilibrium constants for dehydrogenation and protonation elementary steps. To minimize the number of model parameters, the kinetic and thermodynamic constants are defined as functions of the chain length. Vapor–liquid equilibrium is calculated along the reactor, and the hydrocarbons concentrations are described by means of fugacity. The model provides quite a good fitting of experimental results and is able to predict the effects of the operating conditions (temperature, pressure, H_2/wax ratio, and WHSV). Outstandingly, the estimated values and trends of the kinetic and thermodynamic constants (activation energies, Langmuir adsorption constants, etc.) are in line with their physical meaning. © 2010 American Institute of Chemical Engineers *AIChE J,* 57: 711–723, 2011

Keywords: lumped kinetics, mathematical modeling, phase equilibria, hydrocracking, Fischer-Tropsch waxes, paraffins

Introduction

The hydrocracking (HDK) of *n*-paraffins over bifunctional catalysts has been studied intensively, mainly on model compounds. In particular, Weitkamp and coworkers have investigated product distribution, with an insight into isomers composition.[1–4] These works are outstanding in the definition of the HDK reaction mechanism, mainly concerning the formation of branched products and C—C bond scission pattern. Later, Froment and coworkers focused on the development of a kinetic model for the HDK reaction of model compounds. The first models, developed in the 1980s, were "lumped kinetics,"[5,6] i.e., the reaction products were divided into main classes, or lumps, namely *n*-paraffins, *iso*-paraffins (sometimes split into mono- and multibranched), and cracked products, according to the simplified scheme:

$$n\text{-paraffin} \leftrightarrows \text{monobranched paraffin} \leftrightarrows \text{multibranched paraffin} \rightarrow \text{cracked products.} \quad (1)$$

According to the generally accepted reaction schemes, the normal paraffin is first adsorbed on the catalyst surface, dehydrogenated at the metal sites to form the olefin, which migrates to the acid site where the secondary carbenium is formed by protonation of the double bond. The carbenium ion so formed undergoes rearrangement to tertiary carbenium, which in turn can either deprotonate to the corresponding *iso*-olefin or produce lower molecular weight compounds via β-scission. The desorbed olefin formed by deprotonation of

Correspondence concerning this article should be addressed to C. Gambaro at chiara.gambaro@eni.com.

tertiary carbenium migrates to the metal particle to form the saturated compound, which can eventually further react following the scheme presented above.

Apart from more recent works where deviation from ideal HDK has been examined,[7,8] the development of the rate equation is mostly carried out according to the Langmuir-Hinshelwood-Hougen-Watson (LHHW) approach, where the adsorption–desorption as well as the hydrogenation–dehydrogenation steps are assumed to be in quasi-equilibrium, while each step involving the carbenium ion could be a rate-determining step (RDS). Baltanas et al.[6] compared different models obtained by changing the RDS and/or the physisorption isotherm equation: the conclusion drawn by the authors was that the best model corresponds to a dual function, single-site mechanism, with carbenium ion rearrangement as RDS, while among the various adsorption isotherms considered (i.e., Freundlich, Dubinin, Drachsel, and Langmuir) to relate the gas-phase concentrations with those on the catalyst surface, the Langmuir was the best.

When the activity of the metallic hydro/dehydrogenating function makes the olefin formation rate fast enough not to be the limiting step, the acid function determines the kinetic of the system.[9,10] In these circumstances, where the observed conversion rate does not depend on metal concentration, the rearrangement of secondary to tertiary carbenium can be the RDS.

An evolution in the modeling of HDK reaction is represented by the "single-event kinetics"[11,12]: a network of elementary reactions is designed taking into account the formation of each single component of the product mixture. The single events coefficients of elementary steps considered should be independent of the structure of reactant and products and therefore of feedstock composition. However, this approach, if applied without any simplifying assumption, originates a huge number of elementary steps even for relatively simple molecules, which makes its use problematic for more complex mixtures such as Fischer-Tropsch waxes. In recent times, different authors have proposed some strategies to develop detailed mechanistic kinetic models that can be extended to the HDK of mixtures of paraffins. In 2001, Martens and Marin presented a relumped model: eight discrete lumps were identified on the basis of the most relevant classes of hydrocarbons present in an oil fraction. The lumped model coefficients (for reaction rate, physisorption, and vapor–liquid equilibrium) were defined as a combination of the corresponding single-event coefficients, which are independent on the carbon number. This simplification derives from the application of the structure-oriented approach. The kinetic model was coupled with an adiabatic multiphase fixed-bed reactor model for the HDK of VGO.[13]

Kumar and Froment have proposed a generalized mechanistic model for paraffins HDK: the model parameters were estimated from data on HDK of n-$C_{16}H_{34}$; then the tool was applied to the HDK of heavier paraffins. This shift was possible because the rate constants for the elementary steps are independent on the carbon number.[14] The authors state that the model can be easily extended to the HDK of Fischer-Tropsch waxes.

Despite several attempts to make the single-event approach easier to apply, in particular from the point of view of the required computing power, the kinetics of complex mixtures is still preferably described by means of lumping models.[15,16]

Recently, within collaboration between eni and Politecnico di Milano, a kinetic model for the HDK of Fischer-Tropsch waxes based on LHHW formalism has been developed and different, improved versions of that model have been published.[17–20] The "all component" version of the model is able to describe the distribution of the HDK products in the range from C1 to C70, divided into linear and branched products, the latter considered as a unique lump.[18] In an improved version,[19] vapor–liquid equilibrium was accounted for by describing the mixture composition with fugacity. A critical hypothesis of this version is that cracking of the C—C bond is supposed to occur in the middle of the chain. A significant improvement was achieved by introducing a probability function for cracking (instead of the breakage in the middle of the chain).[20] This function has been designed according to literature observations and assumes that the C—C bonds between C_4 and C_{n-4} can be cracked with the same probability (P); the cracking probability of the third and $(n - 3)$th bonds is $P/2$; the cracking probability of the four terminal C—C bonds is 0. The formation of CH_4 and C_2H_6 is accounted for by cracking of C_6H_{14}.[21]

The latter model is considered as starting point for this work. The main goal was to further improve the quality of the fitting and possibly its prediction capability outside the experimental domain used to generate the dataset for the kinetic modeling. Two new versions have been developed: in the first one, all the hypotheses of the model by Gamba et al. were adopted,[20] but different expressions were chosen to correlate the kinetic constants with chain length, and a more complete expression for the isomerization and cracking rates was introduced. In the second version, the complete form for the reaction rate, as reported by Froment,[11] was used. The goal of the work was to develop a kinetic model as much as possible adherent to the chemical–physical nature of the system considered.

Experimental

The experimental data were collected on the HDK unit placed in eni's laboratories. The unit is equipped with a down-flow trickle bed reactor (ID = 16 mm), loaded with 9 g of powdered fresh catalyst. The catalyst is typically a bifunctional system, made of Pt particles dispersed on an amorphous silica–alumina matrix. The extruded particles are crushed and sieved in the range 20–40 mesh (average particle size = 0.625 mm, catalytic bed height = 86 mm) to approximate plug flow behavior. The catalyst was activated in situ by reduction with pure H_2 at high pressure and temperature, according to a standard procedure.

The effect of operating conditions on activity and selectivity was determined by planning the experiments according to a central composite design (CCD).[17] The range of the operating conditions was as follows: temperature = 343–375°C; pressure = 3.5–6 MPa; H_2/wax = 0.06–0.15 g/g; and WHSV = 1–3 h^{-1}. The feedstock used in this study was a paraffinic F-T wax (olefins or alcohols had been removed), whose distribution with chain length is given in Figure 1.

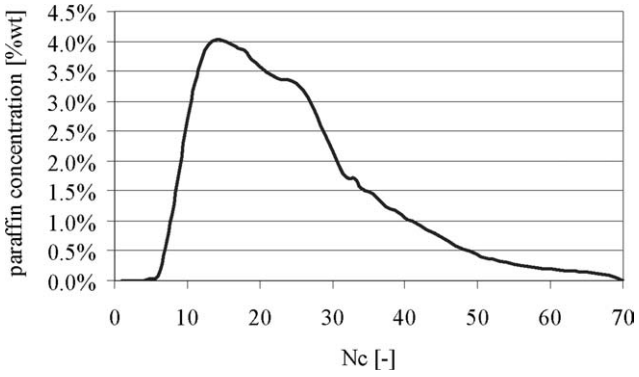

Figure 1. Paraffins distribution with chain length of the Fischer-Tropsch wax used as feedstock for the experiments.

The dataset has already been used for the development of previous versions of the HDK model.[17–20] In this work, the experimental results were analyzed with a code built on the Athena Visual Studio platform: first, model parameters were estimated by means of the DDAPLUS algorithm.[22]

Kinetic Model

Model 1

The most widely accepted reaction mechanism for hydroisomerization and HDK of linear paraffins, which is the basis for the kinetic models present in literature, can be represented by the following set of elementary steps[6]:

(1) $n\text{-P}_n \leftrightarrows n\text{-P}_n^*$ *n*-paraffin adsorption on catalyst surface

(2) $n\text{-P}_n^* \leftrightarrows n\text{-O}_n^* + \text{H}_2$ dehydrogenation on metal site

(3) $n\text{-O}_n^* + \text{H}^+ \leftrightarrows n\text{-R}_n^+$ formation of carbenium ion on acid site

(4) $n\text{-R}_n^+ \leftrightarrows iso\text{-R}_n^+$ carbenium ion rearrangement

(5) $iso\text{-R}_n^+ \leftrightarrows iso\text{-O}_n^* + \text{H}^+$ deprotonation of the carbenium ion

(5′) $iso\text{-R}_n^+ \leftrightarrows n/iso\text{-O}_m^* + \text{R}_{n-m}^+$ β-scission of carbenium ion

(6) $iso\text{-O}_n^* + \text{H}_2 \leftrightarrows iso\text{-P}_n^*$ hydrogenation of the adsorbed *iso*-olefin

(7) $iso\text{-P}_n^* \leftrightarrows iso\text{-P}_n$ desorption of the *iso*-paraffin

Owing to analytical constrains, the HDK kinetic model is based on a more simplified scheme than the one previously shown in (1): in our case, isomers are considered as a unique lump, without distinction between different degrees of branching:

$$n\text{-paraffin} \leftrightarrows iso\text{-paraffin} \rightarrow \text{cracked products.} \quad (2)$$

This simplifying assumption stems from the experimental impossibility of determining the different classes of isomers for the heavier fraction of products. The *n*-paraffin Pn (in the range C5–C70) is isomerized to a pseudo-component, named ''*iso*-paraffin,'' which represents all the isomers of Pn, regardless of the number, position, and length of the branches.

The first hypothesis of the model is that no isomerization takes place with *n*-butane: *iso*-butane is only formed from cracking of heavier molecules. This hypothesis is based on experimental results, and it is most likely the consequence of the operating reaction mechanism in isomerization of type B, which proceeds via protonated cyclopropanes.[23]

The second step is the cracking of the *iso*-paraffin pseudo-component. The mathematical description of the cracking reaction required several hypotheses, mainly based on evidence from scientific literature on hydroisomerization/cracking of model compounds[24]:

(i) *iso*-C5 can be formed like the homologs of higher molecular weight but does not undergo cracking reactions. Such cracking reaction would necessarily involve the passage from a tertiary to a primary carbenium ion, which is particularly disadvantageous from an energetic standpoint, because the primary carbenium would be CH_3^+.

(ii) Only *iso*-paraffins in the range C_6–C_{70} are cracked. This hypothesis is based on results reported by Martens et al.[4] and has been reproposed recently by other authors.[25]

Cracking of *iso*-C_6 via type C scission leads to the formation of propane, but also ethane and methane are formed as reported by Haag and Dessau.[21] Another route for the formation of CH_4 and C_2H_6, which is not considered in this model, is hydrogenolysis of normal and *iso*-paraffins.[26,27] *Iso*-C_7 cracking, via type B1 and B2 scission, gives equimolar quantities of C_3 and *iso*-C_4. For *iso*-paraffins with eight or more carbon atoms, cracking of C—C bonds occurs as explained below (point iv).

(iii) Depending on the type of cracking reaction, cracking of *iso*-paraffin lumps can lead to both *iso*- and *n*-paraffins.

(iv) Cracking of C—C bonds of aliphatic chains with eight or more carbon atoms occurs according to a probability function defined as follows: the C—C bonds between C_4 and C_{n-4} are cracked with the same probability (p); the cracking probability of the third and $(n-3)$th bonds is $p/2$; the cracking probability of the four terminal C—C bonds (i.e., 1st, 2nd, $(n-1)$th, and nth) is 0. This kind of distribution of the cracking probability with chain length is the easiest function to resemble the bell-like cracking products distribution observed experimentally and widely reported in literature for model compounds.[28] As the overall cracking probability equals 1, the cracking probability can be calculated by a simple balance: being n the number of carbon atoms, each molecule has $n-7$ bonds with a cracking probability p, two bonds with a probability $p/2$ and four bonds with null probability of cracking:

$$(n-7)\times p + 2\times p/2 = 1 \Rightarrow (n-6)\times p = 1 \Rightarrow p = 1/(n-6). \quad (3)$$

Each *iso*-paraffin $\geq C_8$ gives rise to $2 \times p$ molecules of each hydrocarbon in the range C_4–C_{n-4} and to $2\times(p/2) = p$ molecules of C_3 and C_{n-3}. This kind of distribution is widely reported in literature to describe the distribution of HDK products.[2,28]

A classical Langmuir-Hinshelwood approach was followed, taking into account the bifunctional nature of the catalyst: hydro–dehydrogenation reactions occur on the metal sites, whereas isomerization and cracking take place on the acid sites of the Si–Al support. Moreover, physisorption of the *n*-paraffin is accounted for and described by means of the Langmuir isotherm. These assumptions are the bases of widely accepted HDK and isomerization models reported in literature.[6]

The overall rate expressions for each component are calculated as combination of three terms: isomerization (r_{iso}),

cracking (r_{ck}), and formation by cracking of a longer molecule (r_{prod}). The rate expressions are defined as follows:

$$r_{isom}(i) = \frac{k_{isom}(i) \times \left(f_n(i) - \frac{f_{iso}(i)}{K_{eq}(i)}\right)}{f_{H_2} \times \left[1 + \sum_{i=1}^{nC} f_n(i) \times K_{L,n}(i) + \sum_{i=4}^{nC} f_{iso}(i) \times K_{L,iso}(i)\right]} \quad (4)$$

$$r_{ck}(i) = \frac{k_{ck}(i) \times f_{iso}(i)}{f_{H_2} \times \left[1 + \sum_{i=1}^{nC} f_n(i) \times K_{L,n}(i) + \sum_{i=4}^{nC} f_{iso}(i) \times K_{L,iso}(i)\right]} \quad (5)$$

$$r_{prod,iso}(i) = \text{Par15} \times \sum_{j=i+4}^{70} \left(\frac{2}{j-6} \times r_{ck}(j)\right) + \left(\frac{2}{2 \times (i+3) - 12} \times r_{ck}(i+3)\right) \quad (6)$$

$$r_{prod,n}(i) = (1 - \text{Par15}) \times \sum_{j=i+4}^{70} \left(\frac{2}{j-6} \times r_{ck}(j)\right) \quad (7)$$

$$r_{prod}(i=3) = \sum_{j=7}^{70} \left(\frac{2}{2 \times (j) - 12} \times r_{ck}(j)\right). \quad (8)$$

The kinetic constants, k_{isom} and k_{ck}, are defined according to a reparametrization of the Arrhenius equation:

$$k(i) = k^{\circ}(i) \times \exp\left[-\frac{E(i)}{R} \times \left(\frac{1}{T} - \frac{1}{T_{ref}}\right)\right]. \quad (9)$$

This form is often used to simplify the estimation of k° and E by breaking the correlation between them.[5,6] Notably, three formation rates are defined, one for *iso*-paraffins, one for *n*-paraffins, and the last one for propane. The formation rate is the sum of the products between the cracking rate and a stoichiometric coefficient calculated from the probability function for all *iso*-paraffins that are susceptible to cracking. The term Par15 represents the *iso*-paraffins fraction (*iso*/*n* + *iso*) that can be obtained from cracking of a generic *iso*-paraffin.

This kinetic model is coupled with the reactor model, considered as an ideal plug flow reactor. Like in the so-called "all components" model,[18] 138 material balance equations are defined, one for each component (70 *n*-paraffins, 67 *iso*-paraffins and H_2):

$$\frac{dY_{isoC}(i)}{d\tau} = -r_{iso}(i) + r_{prod,iso}(i) - r_{cr} \quad i = 6,70 \quad (10)$$

$$\frac{dY_{nC}(i)}{d\tau} = r_{iso}(i) + r_{prod,n}(i) \quad i = 6,70 \quad (11)$$

$$\frac{dY_{isoC}(5)}{d\tau} = -r_{iso}(5) + r_{prod,iso}(5) \quad (12)$$

$$\frac{dY_{nC}(5)}{d\tau} = r_{iso}(5) + r_{prod,n}(5) + \frac{2}{5} \times r_{cr}(6) \quad (13)$$

$$\frac{dY_{isoC}(4)}{d\tau} = r_{prod,iso}(4) \quad (14)$$

$$\frac{dY_{nC}(i)}{d\tau} = r_{prod,n}(i) + \frac{2}{5} \times r_{cr}(6) \quad i = 3,4 \quad (15)$$

$$\frac{dY_{nC}(i)}{d\tau} = \frac{2}{5} \times r_{cr}(6) \quad i = 1,2 \quad (16)$$

$$\frac{dY_{H_2}}{d\tau} = \sum_{i=6}^{70} r_{cr}(i). \quad (17)$$

Vapor–liquid equilibrium is accounted for by introducing the fugacity for each component.[19] Fugacity of each molecule in the reaction mixture (paraffins and H_2) is estimated by means of vapor–liquid equilibrium calculations, using the Redlich-Kwong-Soave cubic equation of state. Flash calculations are performed at the reactor inlet and at nine points along the length of the catalytic bed.

The use of this approach to model the HDK process would require estimation of hundreds of kinetic parameters, which would be statistically meaningless considering that the number of experiments carried out in this case equals 47 (i.e., 25 of CCD plus repetitions of the central point and some other points of experimental plan). To lower the number of parameters to be estimated, kinetic and thermodynamic model constants were expressed as a function of chain length in a sort of "continuous lumping" approach. Obviously, the fitting capability and meaning of the esteemed kinetic parameters significantly depend on the "goodness" of the chosen functions.

This first model is similar to the one described by Gamba et al.[20] The major novelty is represented by the functions used to correlate the kinetic and thermodynamic constants with paraffin chain length. In particular, the dependency of the adsorption (or Langmuir) constants from chain length is expressed by a hyperbolic tangent (Eqs. 18 and 20), because it can change its shape, ranging from a sigmoid to an exponential-like function, according to the values of its coefficients. Furthermore, an "S-like" evolution of K_L with carbon number seems likely according to several evidences reported in literature. The preexponential factors and the activation energies for the isomerization and cracking reactions are power functions of i (Eqs. 22–25). The isomerization equilibrium constant was defined as a continuous, quadratic function ($y = ax^2 + bx + c$), forced through the point ($x = 3$; $y = 0$), for obvious reasons (Eq. 26). This correlation was chosen because the optimization with Athena failed when a power or an exponential function was introduced.

The following set of equations was obtained:

$$K_{L,n}(\text{i}) = 0.1 \times \text{Par1} \times (\text{th}_n(i) + 1) \quad (18)$$

with

$$\text{th}_n(i) = \frac{\exp(i \times \text{Par2} - 2) - \exp(-(i \times \text{Par2} - 2))}{\exp(i \times \text{Par2} - 2) + \exp(-(i \times \text{Par2} - 2))} \quad (19)$$

$$K_{L,iso}(i) = 0.1 \times \text{Par3} \times (\text{th}_{iso}(i) + 1) \quad (20)$$

with

$$\text{th}_{iso}(i) = \frac{\exp(i \times \text{Par4} - 2) - \exp(-(i \times \text{Par4} - 2))}{\exp(i \times \text{Par4} - 2) + \exp(-(i \times \text{Par4} - 2))} \quad (21)$$

Table 1. Results of the Optimization of Model 1: Estimated Parameters and Statistical Analysis

Asymptotic Statistical Analysis					
R-square			0.958		
Adjusted *R*-square			0.957		
Residual sum of squares			1.59×10^{3}		
Average absolute residual			1.44		
Akaike information criterion			1.38		
Parameter	User Estimates	Optimal Estimates	*t*-Value	Standard Deviation	Asymptotic 95% Confidence Intervals
PAR(1) = $P(K_{L,n})$	8.46×10^{1}	8.43×10^{1}	6.41×10^{1}	1.32×10^{0}	$8.43 \times 10^{1} \pm 2.60 \times 10^{0}$
PAR(2) = $P(K_{L,n})$	2.71×10^{-1}	2.51×10^{-1}	1.48×10^{2}	1.70×10^{-3}	$2.51 \times 10^{-1} \pm 3.36 \times 10^{-3}$
PAR(3) = $P(K_{L,iso})$	3.98×10^{1}	4.61×10^{1}	1.25×10^{3}	3.68×10^{-2}	$4.61 \times 10^{1} \pm 7.26 \times 10^{-2}$
PAR(4) = $P(K_{L,iso})$	1.10×10^{-1}	1.10×10^{-1}			
PAR(5) = $P(E_{isom})$	2.92×10^{4}	3.40×10^{4}	1.98×10^{1}	1.72×10^{3}	$3.40 \times 10^{4} \pm 3.38 \times 10^{3}$
PAR(6) = $P(E_{isom})$	4.63×10^{-1}	3.89×10^{-1}			
PAR(7) = $P(E_{ck})$	4.02×10^{4}	4.11×10^{4}	5.60×10^{0}	7.33×10^{3}	$4.11 \times 10^{4} \pm 1.45 \times 10^{4}$
PAR(8) = $P(E_{ck})$	5.10×10^{-1}	5.09×10^{-1}	1.09×10^{1}	4.68×10^{-2}	$5.09 \times 10^{-1} \pm 9.23 \times 10^{-2}$
PAR(9) = $P(k^{\circ}_{isom})$	3.19×10^{-4}	2.98×10^{-4}			
PAR(10) = $P(k^{\circ}_{isom})$	5.00×10^{0}	5.01×10^{0}	1.86×10^{4}	2.69×10^{-4}	$5.01 \times 10^{0} \pm 5.31 \times 10^{-4}$
PAR(11) = $P(k^{\circ}_{ck})$	2.50×10^{-4}	2.53×10^{-4}	1.41×10^{2}	1.80×10^{-6}	$2.53 \times 10^{-4} \pm 3.55 \times 10^{-6}$
PAR(12) = $P(k^{\circ}_{ck})$	4.68×10^{0}	4.68×10^{0}	3.17×10^{3}	1.48×10^{-3}	$4.68 \times 10^{0} \pm 2.91 \times 10^{-3}$
PAR(13) = $P(K_{eq})$	2.00×10^{2}	1.04×10^{2}			
PAR(14) = $P(K_{eq})$	1.00×10^{3}	1.53×10^{3}			
PAR(15) = *iso/n + iso*	8.58×10^{-1}	8.78×10^{-1}	9.16×10^{3}	9.58×10^{-5}	$8.78 \times 10^{-1} \pm 1.89 \times 10^{-4}$

$$E_{isom}(i) = \text{Par5} \times i^{\text{Par6}} \tag{22}$$

$$E_{ck}(i) = \text{Par7} \times i^{\text{Par8}} \tag{23}$$

$$k^{\circ}_{isom}(i) = \text{Par9} \times i^{\text{Par10}} \tag{24}$$

$$k^{\circ}_{ck}(i) = \text{Par11} \times i^{\text{Par12}} \tag{25}$$

$$K_{eq}(i) = \text{Par13} \times \left(i^2 - 9\right) + \text{Par14} \times (i - 3) \tag{26}$$

The model has 15 parameters that were estimated by regression of the experimental data collected, as explained in the "Experimental" section.

Model 2

The second model was developed from the first one, but the isomerization and cracking rates as defined in Eqs. 4 and 5 were substituted by the complete form of the reaction rate according to the Langmuir-Hinshelwood approach[11]:

$$r_{isom}(i) = \frac{k_{isom}(i) \times \left(f_n(i) - \frac{f_{iso}(i)}{K_{eq}(i)}\right)}{f_{H_2} \times \left[1 + \sum_{i=1}^{nC} f_n(i) \times K_{L,n}(i) + \sum_{i=4}^{nC} f_{iso}(i) \times K_{L,iso}(i)\right] + K_{PD}(i) \times \left(K_{L,n}(i) \times f_n(i) + K_{L,iso}(i) \times f_{iso}(i)\right)} \tag{27}$$

$$r_{ck}(i) = \frac{k_{ck}(i) \times f_{iso}(i)}{f_{H_2} \times \left[1 + \sum_{i=1}^{nC} f_n(i) \times K_{L,n}(i) + \sum_{i=4}^{nC} f_{iso}(i) \times K_{L,iso}(i)\right] + K_{PD}(i) \times \left(K_{L,n}(i) \times f_n(i) + K_{L,iso}(i) \times f_{iso}(i)\right)}. \tag{28}$$

For light paraffins, it was demonstrated before that simplified forms (see Eqs. 4 and 5) are as good as the complete equation.[5,6,11] This was explained by considering that for light paraffins, the concentration of carbenium ions is negligible with respect to the overall number of active sites.[11] However, recent results suggest that with relatively long-chain paraffins (*n*-$C_{16}H_{34}$ and *n*-$C_{28}H_{58}$,[29]), the term $K_{PD}(i) \times (K_{L,n}(i) \times f_n(i) + K_{L,iso}(i) \times f_{iso}(i))$ is no longer negligible and the complete form of the equation should be used. Similar results have been obtained by Ribeiro et al.[30] observing fractional reaction orders for both H_2 and *n*-hexane during hydroisomerization of the paraffin on Pt/zeolites. Thus, the contribution of the paraffin concentration is not negligible with respect to the H_2 concentration. This surprising result, in contrast to what is generally reported in literature for Pt/silica–alumina catalysts, was accounted for by using the complete form of the Langmuir rate expression.[5,31,32]

The new constant, K_{PD}, represents the product of the equilibrium constants for dehydrogenation and protonation elementary steps. Hence, the distinction between protonation and chemisorption as RDS is not critical in the present model. K_{PD} is defined as a power function of the number of carbon atoms of the molecule:

$$K_{PD}(i) = \text{Par16} \times \text{i}^{\text{Par17}}. \tag{29}$$

Results and Discussion

The estimated model parameters for Models 1 and 2 are reported, along with some statistics, in Tables 1 and 2, respectively. In both cases, the fitting is quite good, because

Table 2. Results of the Optimization of Model 2: Estimated Parameters and Statistical Analysis

Asymptotic Statistical Analysis					
R-square			0.965		
Adjusted R-square			0.964		
Residual sum of squares			1.33×10^{3}		
Average absolute residual			1.34		
Akaike information criterion			1.23		
Parameter	User Estimates	Optimal Estimates	t-Value	Standard Deviation	Asymptotic 95% Confidence Intervals
PAR(1) = $P(K_{L,}n)$	7.91×10^{1}	8.02×10^{1}	5.93×10^{1}	1.35×10^{0}	$8.02 \times 10^{1} \pm 2.67 \times 10^{0}$
PAR(2) = $P(K_{L,n})$	2.20×10^{-1}	2.08×10^{-1}	1.53×10^{2}	1.36×10^{-3}	$2.08 \times 10^{-1} \pm 2.68 \times 10^{-3}$
PAR(3) = $P(K_{L,iso})$	3.59×10^{1}	3.48×10^{1}	3.99×10^{1}	8.73×10^{-1}	$3.48 \times 10^{1} \pm 1.72 \times 10^{0}$
PAR(4) = $P(K_{L,iso})$	1.07×10^{-1}	1.00×10^{-1}	5.54×10^{1}	1.81×10^{-3}	$1.00 \times 10^{-1} \pm 3.57 \times 10^{-3}$
PAR(5) = $P(E_{isom})$	3.12×10^{4}	4.53×10^{4}	1.75×10^{1}	2.58×10^{3}	$4.53 \times 10^{4} \pm 5.10 \times 10^{3}$
PAR(6) = $P(E_{isom})$	5.06×10^{-1}	3.22×10^{-1}	1.29×10^{2}	2.49×10^{-3}	$3.22 \times 10^{-1} \pm 4.91 \times 10^{-3}$
PAR(7) = $P(E_{ck})$	4.00×10^{4}	4.31×10^{4}	8.10×10^{2}	5.32×10^{1}	$4.31 \times 10^{4} \pm 1.05 \times 10^{2}$
PAR(8) = $P(E_{ck})$	5.34×10^{-1}	5.14×10^{-1}	2.39×10^{2}	2.15×10^{-3}	$5.14 \times 10^{-1} \pm 4.24 \times 10^{-3}$
PAR(9) = $P(k^{\circ}_{isom})$	2.78×10^{-4}	2.86×10^{-4}	4.31×10^{2}	6.65×10^{-7}	$2.86 \times 10^{-4} \pm 1.31 \times 10^{-6}$
PAR(10) = $P(k^{\circ}_{isom})$	5.03×10^{0}	5.02×10^{0}	6.90×10^{2}	7.28×10^{-3}	$5.02 \times 10^{0} \pm 1.44 \times 10^{-2}$
PAR(11) = $P(k^{\circ}_{ck})$	2.52×10^{-4}	2.45×10^{-4}			
PAR(12) = $P(k^{\circ}_{ck})$	4.66×10^{0}	4.66×10^{0}	9.60×10^{3}	4.85×10^{-4}	$4.66 \times 10^{0} \pm 9.57 \times 10^{-4}$
PAR(13) = $P(K_{eq})$	4.02×10^{1}	6.62×10^{1}			
PAR(14) = $P(K_{eq})$	2.36×10^{3}	5.55×10^{2}	8.58×10^{-2}	6.47×10^{3}	$5.55 \times 10^{2} \pm 1.28 \times 10^{4}$
PAR(15)=*iso*/*n* + *iso*	8.97×10^{-1}	9.03×10^{-1}	1.24×10^{3}	7.29×10^{-4}	$9.03 \times 10^{-1} \pm 1.44 \times 10^{-3}$
PAR(16) = $P(K_{PD})$	1.49×10^{1}	1.82×10^{1}	8.98×10^{1}	2.03×10^{-1}	$1.82 \times 10^{1} \pm 4.00 \times 10^{-1}$
PAR(17) = $P(K_{PD})$	9.40×10^{-1}	9.59×10^{-1}	6.47×10^{1}	1.48×10^{-2}	$9.59 \times 10^{-1} \pm 2.93 \times 10^{-2}$

high values were obtained for R^2 (>0.95); all parameters were optimized and many of them are statistically significant (10 over 15 in Model 1 and 15 over 17 in Model 2). Notably, the differences between the values of R^2 and adjusted R^2 are very small in both regressions: this suggests that there are no redundant parameters in the models. As a consequence, the improvements achieved with Model 2 (e.g., R^2 increased from 0.958 to 0.965) are not a consequence of the higher number of parameters.

Model discrimination is also possible comparing the "average absolute residuals" (AAR): among rival models, the one with the lowest AAR is the best. This criterion indicates Model 2 as the best.

In the case of nested models, discrimination could be also done by means of the F-test[33]:

$$F\text{-value} = \frac{\frac{\text{residSS}_1 - \text{residSS}_2}{p_2^* - p_1^*}}{\frac{\text{residSS}_2}{n \times v - p_2^*}}, \tag{30}$$

where residSS indicates the residuals sum of squares for Models 1 and 2, respectively, p^* is the number of estimated parameters (10 for Model 1 and 15 for Model 2), n is the number of experiments (47), and v is the number of responses (9). The null hypothesis, that Model 2 does not fit the data better than Model 1, is rejected if F-value is greater than F-table (here, 3.84). In this case, F-value = 15.95, thus Model 2 is better.

A more accurate parameter to discriminate between the models is the Akaike information criterion (AIC):

$$\text{AIC} = p^* \times \frac{2}{n^*} + \ln\left(\frac{\text{RSS}}{n^*}\right) + p^* \times \frac{2}{n^*} \times \frac{p^* + 1}{n^* - p^* - 1}, \tag{31}$$

where n^* is the number of experimental points (product of number of observation times the number of responses, 423), w_i are the weights applied to each point (here, $w_i = 1$ for both models), RSS is the residual sum of squares, and p^* is the number of estimated parameters.

When comparing two models with different numbers of parameters, the index takes into account both the statistical goodness of fit and the number of parameters that have to be estimated to achieve this particular degree of fit, by imposing a penalty for increasing the number of parameters to determine how much better the fitting should be to consider the model with more parameters more appropriate. The most appropriate model is the one with the smallest value.[34] The AIC for Models 1 and 2 are 1.38 (Table 1) and 1.23 (Table 2). All the criteria reported confirm that the higher R^2 in the second model does not merely originate from the use of a higher number of parameters, but rather from a higher statistical significance. Moreover, the result implicitly suggests that the use of the complete form of the rate expression is important when modeling the HDK of long-chain paraffins.

To better appreciate the improvements introduced by the two versions of the model presented here, the calculated product distributions (expressed as mass fraction) are compared to the experimental ones. Data relative to tests at different conditions are presented in Figures 2–6.

Generally speaking, both models describe quite well the experimental data, in particular in the middle distillates region (C10–C22). Notably, Model 2 provides a better prediction of the results and in many cases the observed and predicted distributions overlap. The improvement is particularly evident for the isomers distributions at the lower conversions (8.6 and 24.2%, Figures 2 and 3, respectively). As for the goodness of fitting of different distillation cuts, the best agreement between experimental and esteemed results is observed for kerosene (C10–14), gas oil (C15–22), and atmospheric residue (C22+): the parity plots relative to these cuts obtained with Model 2 are shown in Figures 7 and 8.

For the lighter fractions, C1–4 and C5–9, the goodness of fitting is less satisfactory. Besides the simplifying assumption concerning the products distribution and the route for the formation of methane and ethane, a possible cause for

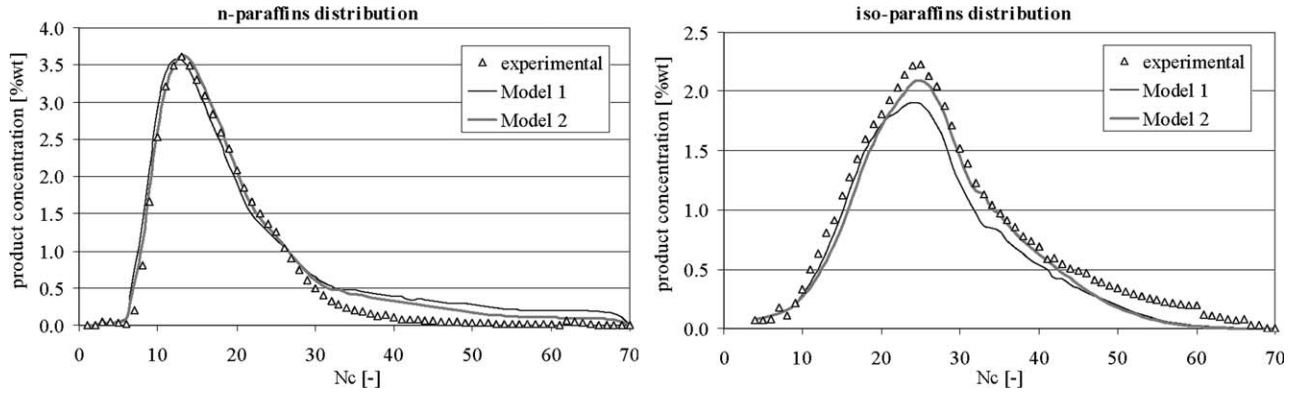

Figure 2. Product distribution, as *n*-paraffins (left) and *iso*-paraffins (right) weight percent, in a test at C_{22+} conversion = 8.6% (experimental).

Experimental data and results obtained with Models 1 and 2. Operating conditions: $T = 343°C$, $P = 4.75$ MPa, H_2/wax = 0.105 g/g, and WHSV = 2.0 h^{-1}.

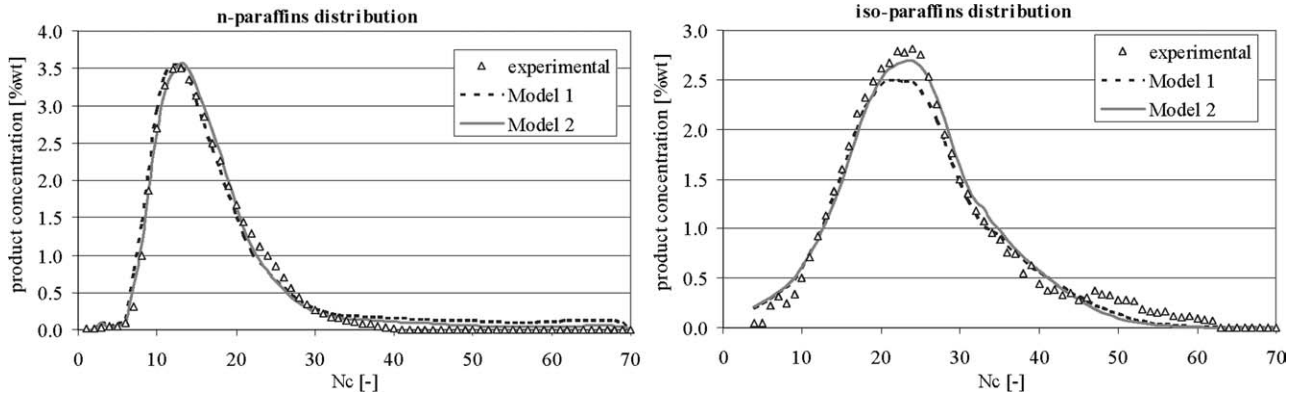

Figure 3. Product distribution, as *n*-paraffins (left) and *iso*-paraffins (right) weight percent, in a test at C_{22+} conversion = 24.2% (experimental).

Experimental data and results obtained with Models 1 and 2. Operating conditions: $T = 351°C$, $P = 4.75$ MPa, H_2/wax = 0.105 g/g, and WHSV = 2.0 h^{-1}.

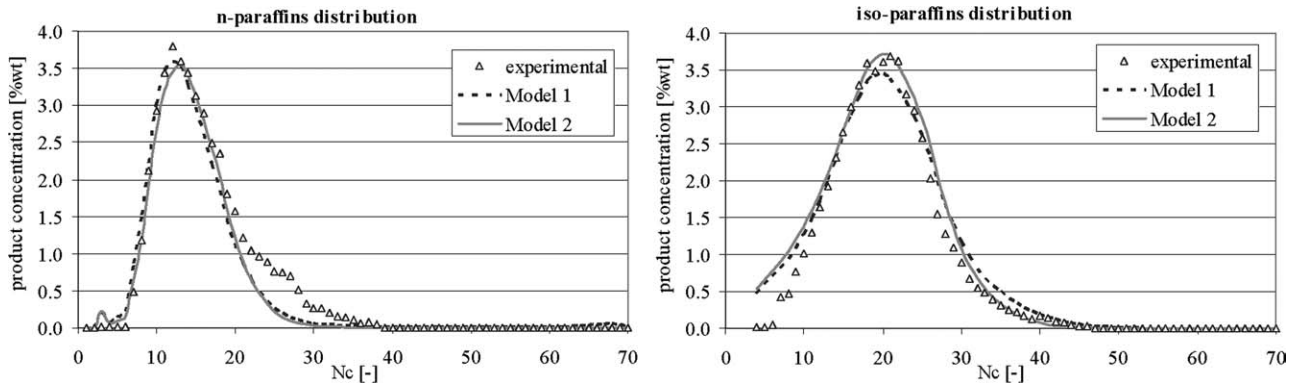

Figure 4. Product distribution, as *n*-paraffins (left) and *iso*-paraffins (right) weight percent, in a test at C_{22+} conversion = 47.1% (experimental).

Experimental data and results obtained with Models 1 and 2. Operating conditions: $T = 359°C$, $P = 4.75$ MPa, H_2/wax = 0.105 g/g, and WHSV = 2.0 h^{-1} (reference run).

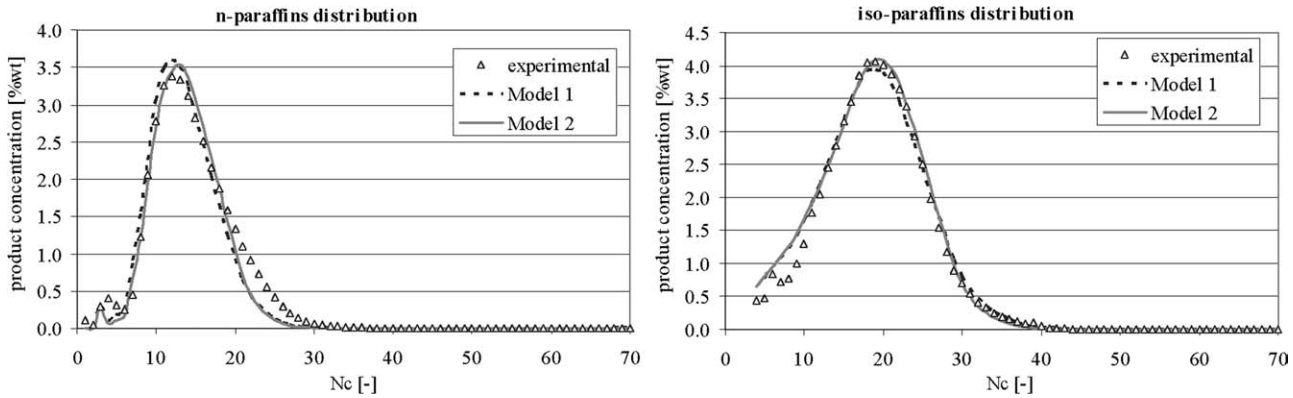

Figure 5. Product distribution, as *n*-paraffins (left) and *iso*-paraffins (right) weight percent, in a test at C_{22+} conversion = 60.9% (experimental).

Experimental data and results obtained with Models 1 and 2. Operating conditions: $T = 359°C$, $P = 4.125$ MPa, H_2/wax = 0.105 g/g, and WHSV = 2.0 h^{-1}.

the lower goodness of fit for the lighter fractions could lie in the much lower variance of data in comparison with the heavier fractions. In these circumstances, the system tends to minimize preferentially the square difference between the observed and calculated values of those data presenting a higher variance. A possible improvement in this sense could be achieved using coded data to give the same weight to each fraction.

Another important facet is the physical meaning of the kinetic and thermodynamic constants of the models calculated with the parameters estimated. As an example, the activation energies, the kinetic constants, and the Langmuir constants calculated for Model 2 are reported in Figures 9–11. Values reported in literature indicate that the energy of activation of isomerization and cracking are similar, do not show significant variation with chain length, and range between 85 and 125 kJ/mol.[11,34,35] The very similar values determined for isomerization and cracking are considered a proof that they share a common intermediate. In our case, the data plotted in Figure 9 show that the activation energy for isomerization slightly depends on chain length, and the range of values is close to the data published. Differently, the activation energy for cracking is clearly overestimated, particularly for the longest paraffinic chains. Notably, both are apparent activation energies, defined as the sum of the activation energy for the reaction and the adsorption enthalpy: this fact could explain the dependence to chain length and the differences with literature data.

The kinetic constants (Figure 10) increase exponentially with chain length, in line with literature results[36,37]: this is a consequence of both the function chosen for k° (a power function of N_c) and the exponential dependence of the kinetic constant on the apparent activation energy, due to the Arrhenius equation. Analysis of the correlation matrix shows that the kinetic constants are not correlated.

With respect to the physisorption of hydrocarbons, most experimental studies focus on light paraffins ($N_c < 14$).[36,37] In these works, adsorption is described in terms of Henry constants,[38] which fit the adsorption isotherm in the low pressure region.[39] In our previous model,[20] the Langmuir constant was expressed as an exponential function of chain length: this choice was based on literature work concerning adsorption in gas–solid systems. In this work, a more flexible correlation between K_L and N_c is introduced: in fact, the

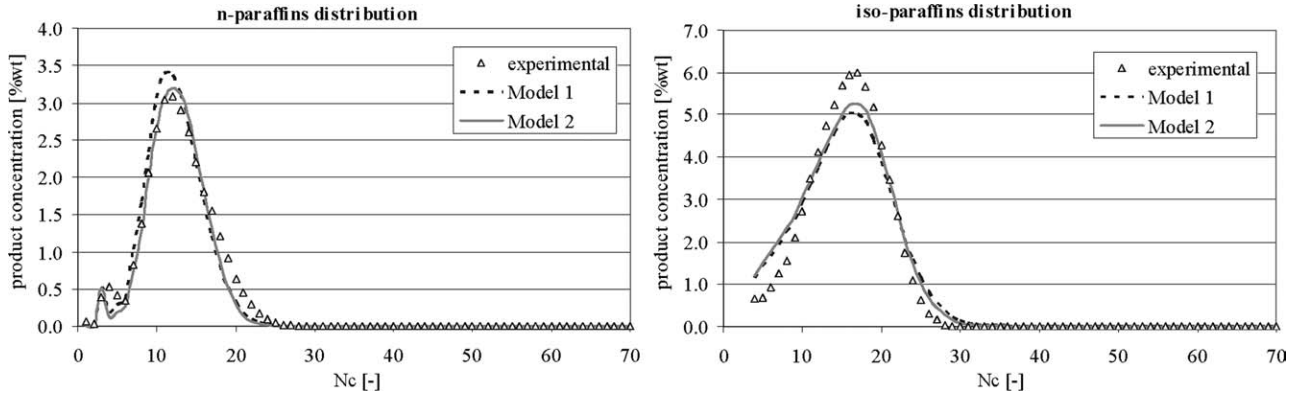

Figure 6. Product distribution, as *n*-paraffins (left) and *iso*-paraffins (right) weight percent, in a test at C_{22+} conversion = 91.3% (experimental).

Experimental data and results obtained with Models 1 and 2. Operating conditions: $T = 359°C$, $P = 4.75$ MPa, H_2/wax = 0.105 g/g, and WHSV = 1.0 h^{-1}.

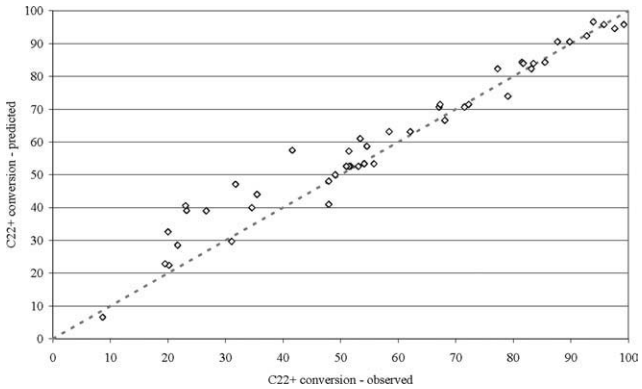

Figure 7. Parity plot for C22+ conversion in the complete dataset (Model 2 results vs. experimental data).

The range of the operating conditions was as follows: temperature = 343–375°C; pressure = 3.5–6 MPa; H_2/wax = 0.06–0.15 g/g; and WHSV = 1–3 h^{-1}.

hyperbolic tangent can change its shape according to the values of its argument (in this case, the values of Par2 and Par4). The optimization of model parameters is such that the Langmuir constants for linear and branched paraffins display a sigmoidal trend (Figure 11). This behavior can also be qualitatively explained in terms of adsorption mechanism. In an ideal trickle-bed reactor, the catalyst is perfectly wetted by the liquid phase. In contrast to what is typically observed in diluted gas-phase conditions, where adsorption constants increase exponentially with carbon number, adsorption of paraffins from a liquid phase into the pores of a mesoporous catalyst occurs in a nonselective way, as the interaction between the adsorbing paraffins and the surface of the catalyst is comparable to the intermolecular interactions between the paraffins in the liquid phase.[40] Thus, the driving force for adsorption is independent of chain length, explaining the constant value for K_L from a certain carbon number on (see Figure 11). The amount adsorbed of a given paraffin is proportional to its concentration in the liquid film surrounding the catalyst pellet. However, the lightest paraffins with low boiling points are mainly present in the gas phase, thus their concentration in liquid phase is low. With increasing carbon number, the tendency to remain in the liquid phase rather than in the gas phase increases strongly. As a result, for light paraffins, the concentration in the liquid film surrounding the catalyst also increases steeply with N_c, until a certain chain length corresponding to a boiling point from where the paraffins are fully present in the liquid phase. Thus, the amount of the lightest paraffins in the pores will be low, leading to a low reaction rate. Heavier paraffins are present in higher concentrations in liquid film and catalyst pores, leading to a higher reaction rate. As the model does not explicitly take the two gas and liquid phases into account, the relative distribution of light and heavy paraffins over both phases is captured in the Langmuir adsorption constants. To describe the lower conversion rate of the lightest paraffins, lower adsorption constants are resulting from the model fitting. For heavy paraffins, which show full liquid behavior, the adsorption constants are not affected by carbon number. As *iso*-paraffins have lower boiling points than the linear paraffins, the plateau in K_L is shifted toward higher carbon numbers.

An esteem of the isomerization equilibrium constant (K_{eq}) is given by Pellegrini et al.[41] The equilibrium constant is defined as a function of temperature, by means of the Gibbs free energy of reaction. The values reported in this article for isomerization of *n*-paraffins to multibranched isomers, at $T = 359°C$, are compared to model results in Table 3. Literature data are well fitted by an exponential function of carbon number ($K_{eq} = 0.0124e^{0.68Nc}$), but this kind of expression generated several problems during parameter estimation, maybe because the increase of K_{eq} with N_c was too fast. A slower function, like a parabola, suited better to our system.

The high value for parameter 15 (0.858 for Model 1 and 0.897 for Model 2), which represents the fraction of *iso*-paraffins formed by cracking, can be explained in the light of the β-scission mechanism.[4] It is generally accepted that type A β-scission is by far the fastest reaction for paraffins $\geq C_8$,[4,24,28] therefore the high value for Par15 would indicate that most of the cracking occurs via type A β-scission. However, if cracking occurred only according to this mechanism, reaction would give only *iso*-paraffins and Par15 (i.e., the fraction of isomers to overall products) would equal 1. Notably, this is not the case, because linear hydrocarbons are

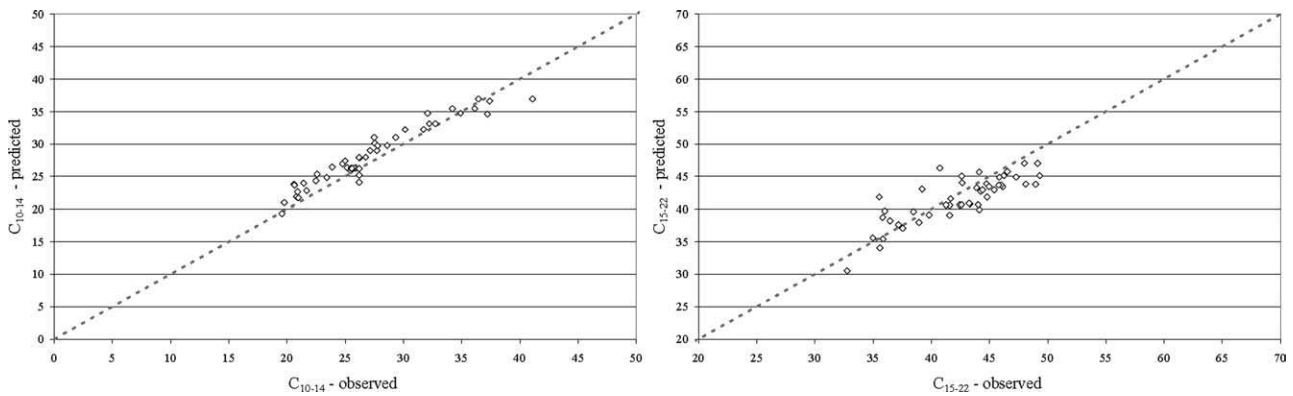

Figure 8. Parity plot for kerosene (left) and gas oil (right) fractions in the complete dataset (Model 2 results vs. experimental data).

The range of the operating conditions was as follows: temperature = 343–375°C; pressure = 3.5–6 MPa; H_2/wax = 0.06–0.15 g/g; and WHSV = 1–3 h^{-1}.

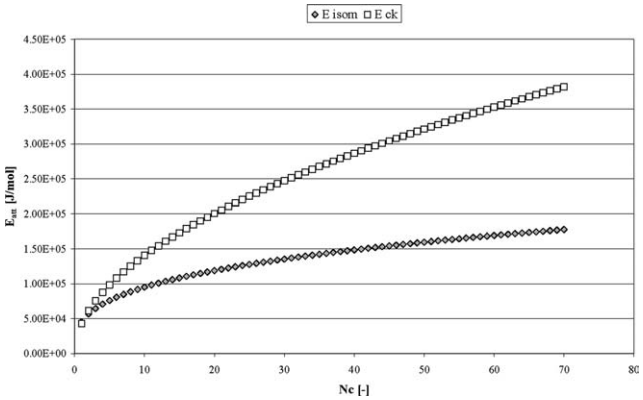

Figure 9. Evolution with carbon number of the activation energies for isomerization (E_{isom}) and cracking (E_{ck}) reactions, calculated with the parameters estimated for Model 2.

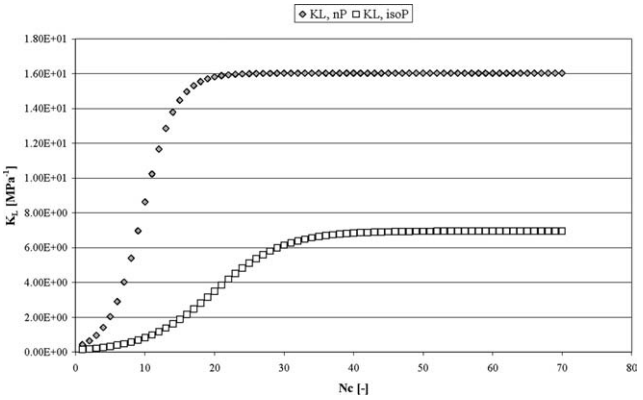

Figure 11. Evolution with carbon number of the Langmuir constants for *n*-paraffins (nP) and *iso*-paraffins (isoP), calculated with the parameters estimated for Model 2.

The range of the operating conditions in the dataset was as follows: temperature = 343–375°C; pressure = 3.5–6 MPa; H_2/wax = 0.06–0.15 g/g; and WHSV = 1–3 h^{-1}.

detected among the cracking products.[2,42,43] This is explained by Martins and coworkers: at increasing the chain length of the feed, the other types of cracking (type B1, B2, and hydrogenolysis) become quantitatively more significant.[4]

In Model 2, parameters 16 and 17 are such that K_{PD} increases almost linearly with the carbon number of the molecule (Par17 $\cong$ 1, see Table 2). This result is in line with expectations: increasing the number of C atoms in the paraffin leads to a higher number of olefins and thus carbenium ions that can be formed. This qualitative observation can be interpreted in terms of entropy, as proposed by de Gauw et al.[44]: the equilibrium constant for dehydrogenation reaction is a function of the entropy of formation of all the olefins that can be obtained from the paraffin Pn:

$$K_{DH} \propto \exp\left(\frac{\Delta S_{f,olefins} - \Delta S_{f,Pn}}{R}\right). \quad (32)$$

The model can also be applied to describe the effect of operating conditions on the main indexes of catalytic performance, namely conversion and selectivity. As an example, in Figure 12 the evolution of C_{22+} conversion as a function of T, P, H_2/wax, and WHSV is reported. The best agreement with experimental data is displayed in the effect of temperature (Figure 12A). The effects of pressure and WHSV (Figures 12B, D) are well fitted at high conversions (>35 wt %), while the lower values are overestimated (the main difference is in the case $P = 6$ MPa). The worse fitted effect is that of the H_2/wax inlet ratio (Figure 12C): the theoretical trace passes only through the central point (as a consequence of the presence of several replicates), while all the other data are overestimated.

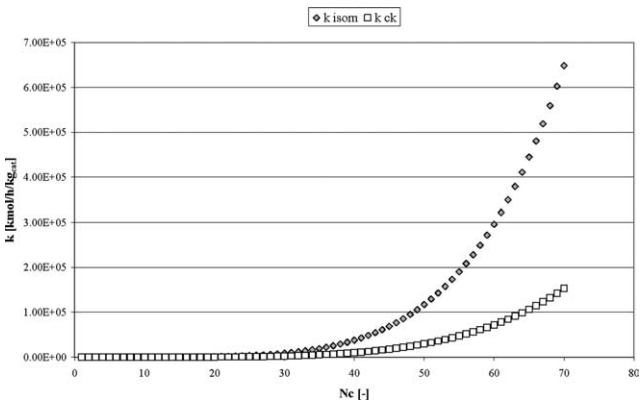

Figure 10. Evolution with carbon number of the kinetic constants for isomerization (k_{isom}) and cracking (k_{ck}) reactions, calculated with the parameters estimated for Model 2 at a temperature of 359°C (temperature of the central point in the experimental design).

Thybaut et al. developed a lumped kinetic model from data on *n*-C_8H_{18}[7]: their model provided a negative (or null) effect of the H_2/paraffin ratio even in the case of a reacting system in nonideal HDK conditions. This result is in contrast to what is experimentally observed during the HDK of complex mixtures.[45] This discrepancy could be explained considering that the physical state of the two systems is different: under typical HDK conditions, light hydrocarbons are in gas phase, while complex mixtures are ruled by vapor–liquid equilibrium. In the former case, an increase in the H_2/feed ratio, at constant total pressure, leads to a decrease in the paraffin partial pressure because of an increase of hydrogen pressure: as a consequence, the numerator of the rate expression decreases, whereas the denominator increases, leading to an overall decrease in the reaction rate. On the contrary, when VLE occurs, an increase in H_2/wax ratio shifts the equilibrium toward the vapor phase, i.e., the hydrocarbons weight fractions in the vapor phase increase, and so does the fugacity, whereas the hydrogen fugacity decreases. Globally, the reaction rate tends to increase, explaining the positive effect of the H_2/feed ratio on conversion.

Conclusions

A kinetic model for the HDK of the Fischer-Tropsch waxes covering a wide range of operating conditions and

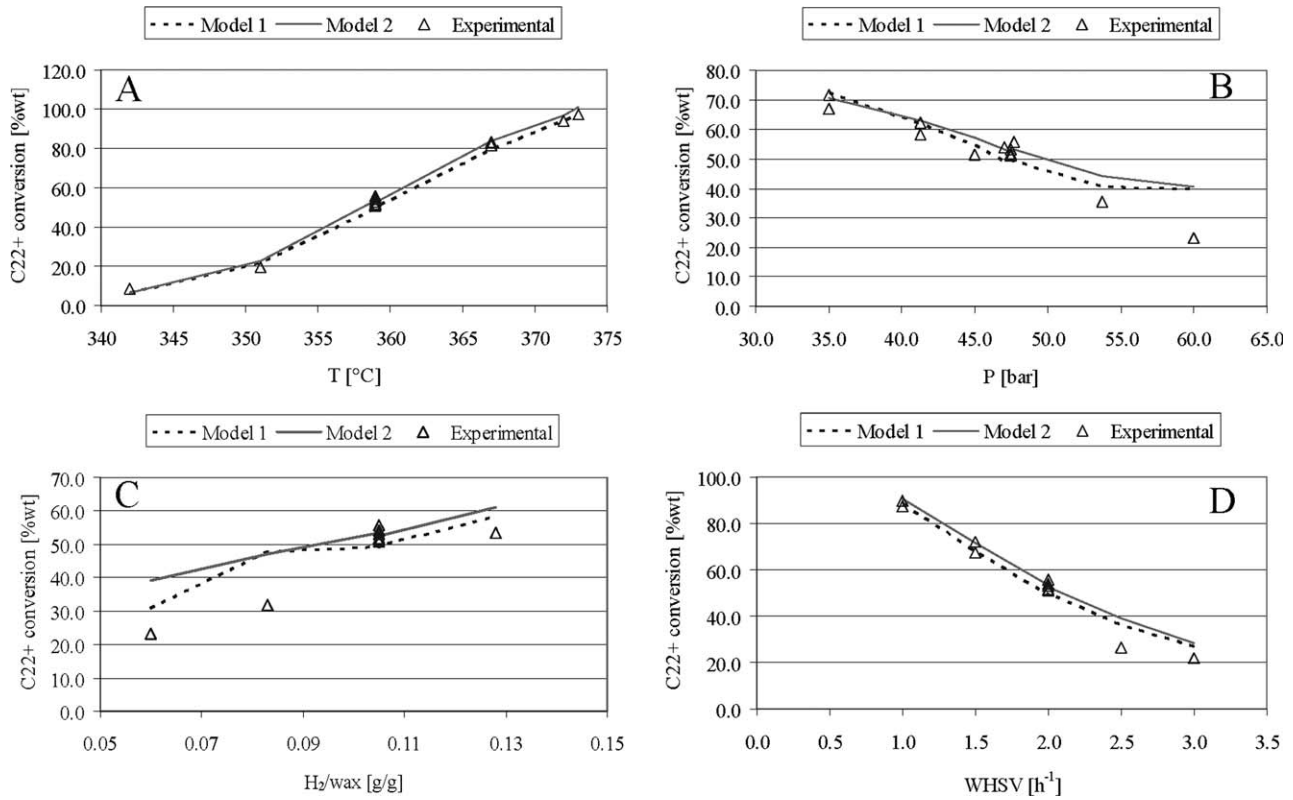

Figure 12. Effect of operating conditions (A: temperature, B: pressure, C: H_2/wax ratio, and D: WHSV) on C_{22+} conversion.

Experimental data are compared with predicted values, calculated with Models 1 and 2.

conversion (8–99%) has been developed. The present model is an improvement of previous work, and the novelty is represented by the correlations between kinetic and thermodynamic constants and the length of the hydrocarbon chain, providing a better fitting of the experimental data (e.g., higher R^2 than in the older versions and better description of the product distribution). Moreover, the introduction of the complete form of the rate expressions for isomerization and cracking (i.e., the addition of the K_{PD} constant) leads to a further improvement of the model (version 2 vs. version 1, presented here) that is not merely the consequence of the higher number of parameters used, but derives from a higher meaningfulness of the model. This result implies that, differently to what observed for light paraffins up to C16, for long-chain paraffins the right-hand term in the denominator of the rate expressions (which contains K_{PD}) is no longer negligible.

Table 3. Estimated (Model) and Published (Literature) Values of the Equilibrium Constant for Isomerization of *n*-Paraffins to Multibranched Isomers

N_c	K_{eq} (Literature)	K_{eq} (Model)
6	7.28×10^{-1}	6.48×10^{3}
7	1.44×10^{0}	9.16×10^{3}
8	3.16×10^{0}	1.21×10^{4}
9	5.93×10^{0}	1.53×10^{4}
10	1.15×10^{1}	1.87×10^{4}
11	2.16×10^{1}	2.25×10^{4}
12	4.19×10^{1}	2.64×10^{4}
13	8.11×10^{1}	3.07×10^{4}
14	1.57×10^{2}	3.52×10^{4}
15	3.11×10^{2}	3.99×10^{4}
16	6.37×10^{2}	4.49×10^{4}
17	1.27×10^{3}	5.02×10^{4}
18	2.58×10^{3}	5.57×10^{4}
19	5.36×10^{3}	6.15×10^{4}
20	1.11×10^{4}	6.76×10^{4}

Literature values[36] correspond to K_{eq} at $T = 359°C$.

Particularly interesting are the results concerning the physisorption of normal and *iso*-paraffins, showing a transition from gas- to liquid-phase behavior which we think mirrors the presence of vapor–liquid equilibrium in the reacting system.[46]

Although the present model provides a quite good agreement with experimental results, especially as for the middle distillates and conversion of C22+ fraction, the model fitting ability could be further improved trying to better predict the effects of operating conditions and the lightest product distribution. Improvements could be obtained by considering:

- the presence of hydrogenolysis (formation of methane and ethane)
- a more realistic products distribution
- explicit description of the gas and liquid phase, as already proposed in some works,[47] and introduction of the wetting factor, which is a critical parameter in trickle-bed reactors, in particular at the highest conversion levels.[48–50]

Moreover, like all the lumping models, the rate parameters are dependent on the feedstock composition.[13] An attempt to overcome this limitation would be extending in the dataset with data collected during HDK of different FT waxes.

Notation

c_P = paraffin concentration in the liquid phase (kmol/kg_{cat})
c_P^* = adsorbed paraffin concentration (kmol/kg_{cat})
c_{sat} = saturation concentration (kmol/kg_{cat})
D_p = catalyst particle diameter (mm)
E = activation energy (J/mol)
f = fugacity (Pa)
H_b = catalyst bed height (mm)
i = index for paraffin chain length
ID = reactor internal diameter (mm)
ΔH° = adsorption enthalpy (J/mol)
k = kinetic constant (kmol/h/kg_{cat})
k° = frequency factor (kmol/h/kg_{cat})
K_{DH} = equilibrium constant for dehydrogenation reaction
K_{eq} = equilibrium constant for isomerization reaction
K_L = Langmuir adsorption constant (MPa^{-1})
K_{PD} = product of the protonation and dehydrogenation constants
N_c = number of carbon atoms
p = cracking probability
r = reaction rate (kmol/kg/h)
R = universal gas constant (kJ/kmol/K)
$S_{f,i}$ = entropy of formation of the species i (J/K)
Y = paraffin to inlet wax ratio ($kmol_i/kg_{wax\ IN}$)

Greek letters

τ = residence time (kg_{cat} h/$kg_{wax,\ IN}$)

Subscripts

ck = cracking reaction
iso = *iso*-paraffin
isom = isomerization (reaction)
n = *n*-paraffin
prod = formation (reaction)

Literature Cited

1. Schulz HF, Weitkamp JH. Zeolite catalysts. Hydrocracking and hydroisomerization of n-dodecane. *Ind Eng Chem Prod Res Dev*. 1972;11:46–53.
2. Steijns M, Froment G, Jacobs P, Uytterhoeven J, Weitkamp J. Hydroisomerization and hydrocracking. II. Product distributions from n-decane and n-dodecane. *Ind Eng Chem Prod Res Dev*. 1981; 20:654–660.
3. Weitkamp J. Isomerization of long-chain n-alkanes on a Pt/CaY zeolite catalyst. *Ind Eng Chem Prod Res Dev*. 1982;21:550–558.
4. Martens JA, Jacobs PA, Weitkamp J. Attempts to rationalize the distribution of hydrocracked products. I. Qualitative description of the primary hydrocracking modes of long chain paraffins in open zeolites. *Appl Catal*. 1986;20:239–281.
5. Steijns M, Froment GF. Hydroisomerization and hydrocracking. III. Kinetic analysis of rate data for n-decane and n-dodecane. *Ind Eng Chem Prod Res Dev*. 1981;20:660–668.
6. Baltanas MA, Vansina H, Froment GF. Hydroisomerization and hydrocracking. V. Kinetic analysis of rate data for n-octane. *Ind Eng Chem Prod Res Dev*. 1983;22:531–539.
7. Thybaut JW, Narasimhan CSL, Denayer JF, Baron GV, Jacobs PA, Martens JA, Maryn GB. Acid-metal balance of a hydrocracking catalyst: ideal versus nonideal behavior. *Ind Eng Chem Res*. 2005;44: 5159–5169.
8. Chavarría-Hernández JC, Ramírez J, Baltanás MA. Single-event-lumped-parameter hybrid (SELPH) model for non-ideal hydrocracking of n-octane. *Catal Today*. 2008;130:455–461.
9. Giannetto GE, Perot GR, Guisnet M. Hydroisomerization and hydrocracking of n-alkanes. I. Ideal hydroisomerization PtHY catalysts. *Ind Eng Chem Prod Res Dev*. 1986;25:481–490.
10. Guisnet M, Alvarez F, Giannetto G, Perot G. Hydroisomerization and hydrocracking of n-heptane on Pth zeolites. Effect of the porosity and of the distribution of metallic and acid sites. *Catal Today*. 1987;1:415–433.
11. Froment GF. Kinetics of the hydroisomerization and hydrocracking of paraffins on a platinum containing bifunctional Y-zeolite. *Catal Today*. 1987;1:455–473.
12. Baltanas MA, Van Raemdonck KK, Froment GF, Mohedas SR. Fundamental kinetic modeling of hydroisomerization and hydrocracking on noble metal-loaded faujasites. I. Rate parameters for hydroisomerization. *Ind Eng Chem Res*. 1989;28:899–910.
13. Martens GG, Marin GB. Kinetics for hydrocracking based on structural classes: model development and application. *AIChE J*. 2001; 47:1607–1622.
14. Kumar H, Froment GF. A Generalized mechanistic kinetic model for the hydroisomerization and hydrocracking of long-chain paraffins. *Ind Eng Chem Res*. 2007;46:4075–4090.
15. Basak K, Sau M, Manna U, Verma RP. Industrial hydrocracker model based on novel continuum lumping approach for optimization in petroleum refinery. *Catal Today*. 2004;98:253–264.
16. Ancheyta J, Sánchez S, Rodríguez MA. Kinetic modeling of hydrocracking of heavy oil fractions: a review. *Catal Today*. 2005;109: 76–92.
17. Pellegrini L, Locatelli S, Rasella S, Bonomi S, Calemma V. Modeling of Fischer-Tropsch products hydrocracking. *Chem Eng Sci*. 2004;59:4781–4787.
18. Pellegrini L, Bonomi S, Gamba S, Calemma V, Molinari D. The "all components hydrocracking model". *Chem Eng Sci*. 2007;62: 5013–5020.
19. Pellegrini L, Gamba S, Calemma V, Bonomi S. Modelling of hydrocracking with vapour-liquid equilibrium. *Chem Eng Sci*. 2008;63: 4285–4291.
20. Gamba S, Pellegrini L, Calemma V, Gambaro C. Introduction of a breakage probability function in the hydrocracking reactor model. *Ind Eng Chem Res*. 2009;48:5656–5665.
21. Haag WO, Haag WC, Dessau RM. Duality of mechanism in acid-catalyzed paraffin cracking. In *Proceedings of the 8th International Congress on Catalysis*, Vol. 2. Weinheim: Verlag Chemie, 1984:II-305–II-313.
22. Caracotsios M, Stewart WE. Sensitivity analysis of initial value problems with mixed ades and algebraic equations. *Comput Chem Eng*. 1985;9:359–365.
23. Brouwer DM, Oelderik JM. HF SbF5 catalysed Isomerization of 2-methyl-pentane. *Recl Trav Chim Pays Bas*. 1968;87:721–736.
24. Marcilly C. *Catalyse Acido-Basique. Application au Raffinage et à la Pétrochimie*. Paris: Editions Technip, 2003.
25. Akhmedov VM, Al-Khowaiter SH. Recent advances and future aspects in the selective isomerization of high n-alkanes. *Catal Rev Sci Eng*. 2007;49:33–139.
26. Bond GC. Kinetic modeling of metal-catalyzed reactions of alkanes. *Ind Eng Chem Res*. 1997;36:3173–3179.
27. Kinger G, Vinek H. n-Nonane hydroconversion on Ni and Pt containing HMFI, HMOR and HBEA. *Appl Catal A*. 2001;218:139–150.
28. Weitkamp J, Jacobs PA, Martens JA. Isomerization and hydrocracking of C9 through C16 n-alkanes on Pt/HZSM-5 zeolite. *Appl Catal*. 1983;8:123–141.
29. Rossetti I, Gambaro C, Calemma V. Hydrocracking of long chain linear paraffins. *Chem Eng J*. 2009;154:295–301.
30. Ribeiro F, Marcilly C, Guisnet M. Hydroisomerization of n-hexane on platinum zeolites. I. Kinetic study of the reaction on platinum/Y-zeolite catalysts: influence of the platinum content. *J Catal*. 1982; 78:267–274.
31. Garin F, Gault FG. Mechanisms of hydrogenolysis and isomerization of hydrocarbons on metals. VIII. Isomerization of carbon-13 labeled pentanes on a 10% platinum-aluminum oxide catalyst. *J Am Chem Soc*. 1975;97:4466–4476.

32. Akhmedov VM, Klabunde KJ. High-activity Re-Pt/MO catalysts for C-C bond cleavage reactions: preparation by solvated metal atom dispersion (SMAD). *J Mol Catal*. 1988;45:193–206.
33. http://en.wikipedia.org/wiki/F-test#cite_note-3.
34. http://www.modelselection.org/aic/.
35. Calemma V, Peratello S, Perego C. Hydroisomerization and hydrocracking of long chain n-alkanes on Pt/amorphous SiO2-Al2O3 catalyst. *Appl Catal A*. 2000;190:207–218.
36. Debrabandere B, Froment GF. Influence of the hydrocarbon chain length on the kinetics of the hydroisomerization and hydrocracking of n-paraffins. *Stud Surf Sci Catal*. 1997;106:379–389.
37. Denayer JF, Baron GV, Jacobs PA, Martens JA. Competitive physisorption effects in hydroisomerisation of n-alkane mixtures on Pt/Y and Pt/USY zeolite catalysts. *Phys Chem Chem Phys*. 2000;2:1007–1014.
38. Denayer JF, Baron GV, Souverijns W, Martens JA, Jacobs PA. Hydrocracking of n-alkane mixtures on Pt/H-Y zeolite: chain length dependence of the adsorption and the kinetic constants. *Ind Eng Chem Res*. 1997;36:3242–3247.
39. Llewellyn PL, Maurin G. Gas adsorption in zeolites and related materials. *Stud Surf Sci Catal*. 2007;168:555–610.
40. Denayer JF, Bouyermaouen A, Baron GV. Adsorption of alkanes and other organic molecules in liquid phase and in the dense vapor phase: influence of polarity, zeolite topology, and external fluid density and pressure. *Ind Eng Chem Res*. 1998;37:3691–3698.
41. Pellegrini LA, Gamba S, Bonomi S, Calemma V. Equilibrium constants for isomerization of n-paraffins. *Ind Eng Chem Res*. 2007;46: 5446–5452.
42. Vansina H, Baltanas MA, Froment GF. Hydroisomerization and hydrocracking. IV. Product distribution from n-octane and 2,2,4-trimethylpentane. *Ind Eng Chem Prod Res Dev*. 1983;22:526–531.
43. Girgis MJ, Tsao YP. Impact of catalyst metal-acid balance in n-hexadecane hydroisomerization and hydrocracking. *Ind Eng Chem Res*. 1996;35:386–396.
44. de Gauw FJMM, van Grondelle J, van Santen RA. The intrinsic kinetics of n-hexane hydroisomerization catalyzed by platinum-loaded solid-acid catalysts. *J Catal*. 2002;206:295–304.
45. Leckel D. Hydrocracking of iron-catalyzed Fischer-Tropsch waxes. *Energy Fuels*. 2005;19:1795–1803.
46. Correra S, Calemma V, Pellegrini L, Bonomi S. Waxy streams characterisation to perform VLE calculations in hydrocracking process. In: Pierucci S, editor. *Chemical Engineering Transactions*, Vol. 6, 2005. AIDIC Servizi S.r.l., Italy. p. 849–854.
47. Kocis GR, Ho TC. Effects of liquid evaporation on the performance of trickle-bed reactors. *Chem Eng Res Des*. 1986;64:288–291.
48. Ishigaki S, Goto S. Vapor-phase kinetics and its contribution to global three-phase reaction rate in hydrogenation of 1-methylnaphthalene. *Catal Today*. 1999;48:31–40.
49. Al-Dahhan MH, Duduković MP. Pressure drop and liquid holdup in high pressure trickle-bed reactors. *Chem Eng Sci*. 1994;49:5681–5698.
50. Biardi G, Baldi G. Three-phase catalytic reactors. *Catal Today*. 1999; 52:223–234.

Manuscript received Feb. 11, 2010, and revision received Apr. 20, 2010.